Dynamical properties of the synchronization transition

Michel Droz[1] and Adam Lipowski[1,2]
[1]*Department of Physics, University of Geneva, CH 1211 Geneva 4, Switzerland*
[2]*Faculty of Physics, A. Mickiewicz University, 61-614 Poznań, Poland*
(Received 7 November 2002; revised manuscript received 21 January 2003; published 13 May 2003)

We use spreading dynamics to study the synchronization transition (ST) of one-dimensional coupled map lattices (CML's). Recently, Baroni *et al.* [Phys. Rev. E **63**, 036226 (2001)] have shown that the ST belongs to the directed percolation (DP) universality class for discontinuous CML's. This was confirmed by accurate numerical simulations for the Bernoulli map by Ahlers and Pikovsky [Phys. Rev. Lett. **88**, 254101 (2002)]. Spreading dynamics confirms such an identification only for random synchronized states. For homogeneous synchronized states the spreading exponents η and δ are different from the DP exponents but their sum equals the corresponding sum of the DP exponents. Such a relation is typical of models with infinitely many absorbing states. Moreover, we calculate the spreading exponents for the tent map for which the ST belongs to the bounded Kardar-Parisi-Zhang (BKPZ) universality class. The estimation of spreading exponents for random synchronized states is consistent with the hyperscaling relation, while it is inconsistent for the homogeneous ones. Finally, we examine the asymmetric tent map. For small asymmetry the ST remains of the BKPZ type. However, for large asymmetry a different critical behavior appears, with exponents being relatively close to those for DP.

DOI: 10.1103/PhysRevE.67.056204 PACS number(s): 05.45.−a, 05.40.Ca

I. INTRODUCTION

Recently, synchronization of chaotic systems has received considerable attention [1]. These studies are partially motivated by experimental realizations in lasers, electronic circuits, and chemical reactions [2]. An interesting problem concerns synchronization in spatially extended systems [3]. It turns out that in such systems synchronization can be regarded as a nonequilibrium phase transitions. The determination of the universality classes for nonequilibrium phase transitions is a problem much debated in the literature. Thus it is natural to ask whether the synchronization transition (ST) can be incorporated into an already known universality class. For certain cellular automata the synchronized state is actually an absorbing state of the dynamics, and the ST in such a case was found to belong to the directed percolation (DP) universality class [4]. This problem is more subtle for continuous chaotic systems such as, e.g., coupled map lattices (CML's) [5]. For CML's a perfect synchronized state is never reached in finite time, which weakens the analogy with DP.

The problem of the ST for CML's driven by additive spatiotemporal noise has been investigated by Baroni *et al.* [6]. They showed that the ST generally yields two different scenarios according to the values assumed by two dynamical indicators ruling the transition, namely, the propagation velocity of finite perturbations and the so-called transverse Lyapunov exponent. This exponent should become negative for synchronization to occur. When both indicators vanish at the transition point, the critical behavior should generically be described by the so-called bounded Kardar-Parisi-Zhang (BKPZ) universality class [7,8]. When the propagation velocity vanishes while the transverse Lyapunov exponent is negative, the critical behavior should be DP-like. Let us notice that the possibility of a finite propagation velocity with negative Lyapunov exponent is very interesting on its own [9]. Alhers and Pikovsky [10] found essentially that a similar scenario holds for bidirectionally coupled CML's. It was argued that DP critical behavior might emerge for systems with discontinuous local maps [6,10]. It was also suggested that such behavior might appear for continuous maps with sufficiently strong nonlinearities [6].

It is well known that models with a single absorbing state exhibit a DP criticality [11]. At first sight one might think that the synchronized state is unique and that this is the reason for its relation with DP criticality for discontinuous maps. Reexamining the model introduced by Ahlers and Pikovsky [10], we show, however, that there are many synchronized states and they differ with respect to the dynamical properties that are detected with the so-called spreading approach [12]. The spreading exponents that we measure for random synchronized states and a discontinuous (Bernoulli) map take DP values. However, the exponents obtained for homogeneous synchronized states take non-DP values. But these exponents satisfy a certain scaling relation that also holds for some models with infinitely many absorbing states [13]. In addition to that, we measured spreading exponents for the ST belonging to the BKPZ universality class. Our results, obtained for the symmetric tent map, together with previous estimations of other exponents in this universality class, show that the hyperscaling relation is satisfied but only for random synchronized states. For homogeneous synchronized states the spreading exponents do not obey the hyperscaling relation. Finally, we examine the asymmetric tent map. For not too large asymmetry the ST remains of BKPZ type. However, for large asymmetry the nature of the ST changes and the critical exponents that we measured are relatively close to that of DP. This shows that the non-BKPZ behavior appears even for continuous maps.

In Sec. II we define the model and briefly describe the simulation method. The results are presented in Sec. III and a final discussion is given in Sec. IV.

II. MODEL AND SIMULATION METHOD

Our model is the same as the one examined recently by Ahlers and Pikovsky (AP) and consists of two coupled CML's [10]:

$$\begin{pmatrix} u_1(x,t+1) \\ u_2(x,t+1) \end{pmatrix} = \begin{pmatrix} 1-\gamma & \gamma \\ \gamma & 1-\gamma \end{pmatrix} \times \begin{pmatrix} (1+\epsilon\Delta) f(u_1(x,t+1)) \\ (1+\epsilon\Delta) f(u_2(x,t+1)) \end{pmatrix}, \quad (1)$$

where Δv is the discrete Laplacian $\Delta v(x) = v(x-1) - 2v(x) + v(x+1)$. Both space and time are discretized, $x = 1,2,\ldots,L$ and $t = 0,1,\ldots$. Periodic boundary conditions are imposed, $u_{1,2}(x+L,t) = u_{1,2}(x,t)$, and similarly to previous studies we set the intrachain coupling $\epsilon = 1/3$. Varying the interchain coupling γ allows us to study the transition between synchronized and chaotic phases. Local dynamics is specified through a nonlinear function $f(u)$ and several cases will be discussed below.

We introduce a synchronization error $w(x,t) = |u_1(x,t) - u_2(x,t)|$ and its spatial average $w(t) = (1/L)\sum_{x=1}^{L} w(x,t)$. The time average of $w(t)$ in the steady state will be simply denoted as w. In the chaotic phase, realized for sufficiently small $\gamma < \gamma_c$, one has $w > 0$, while in the synchronized phase ($\gamma > \gamma_c$), $w = 0$. Moreover, at criticality, i.e., for $\gamma = \gamma_c$, $w(t)$ is expected to have a power-law decay to zero, $w(t) \sim t^{-\Theta}$. In the stationary state, and for γ approaching the critical value γ_c, one expects that $w \sim (\gamma_c - \gamma)^{\beta}$.

It is well known that spreading dynamics is a very effective method to study phase transitions in models with absorbing states [12,14]. In this method one prepares the model in an absorbing state and then one locally sets the activity and monitors its subsequent evolution. Typical observables in this method are the number of active sites $N(t)$, the probability $P(t)$ that activity survives at least up to time t, and the average square spread of active sites $R^2(t)$. However, as we already mentioned, our model never reaches a perfectly synchronized state in a finite time. To define $P(t)$ we have to introduce a small threshold p and consider a system as "perfectly" synchronized when $w(t) < p$. The estimation of the critical value of the interchain coupling γ_c as well as some exponents seems to be independent of the precise value of p, as long as it remains small. In our calculations we usually used $p = 10^{-10}$.

As for the other observables, we define them in the following, p-independent way:

$$N(t) = \sum_{x=1}^{L} w(x,t) = w(t)L,$$
$$R^2(t) = \frac{1}{w(t)} \sum_{x} w(x,t)(x - x_0)^2, \quad (2)$$

where x_0 denotes the site where the activity was set initially. Let us notice that $N(t)$ is directly related to the order parameter. Moreover, the weighted average in the definition of $R^2(t)$ allows us to take into account only sites where the synchronization error is nonzero. As we will see, such observables do possess a correct asymptotic behavior.

According to general scaling arguments [12], we expect that at criticality (i.e., for $\gamma = \gamma_c$) $w(t) \sim t^{\eta}$, $P(t) \sim t^{-\delta}$, and $R^2(t) \sim t^{z}$. These relations define the critical exponents η, δ, and z.

Note that in general the critical behavior of $w(t) \sim t^{\eta}$ in the spreading method might be different from the nonspreading one $w(t) \sim t^{-\Theta}$ discussed above. Moreover, these exponents obey the following hyperscaling relation [14]:

$$\eta + \delta + \Theta = \frac{dz}{2}. \quad (3)$$

III. RESULTS

A. Bernoulli map

First, let us consider the case when $f(u)$ is a Bernoulli map, namely, $f(u) = 2u \pmod 1$ and $0 \leqslant u \leqslant 1$. Measuring w in the steady state and its time dependence $w(t)$, AP concluded that the synchronization transition in this case takes place at $\gamma = \gamma_c = 0.2875(1)$ and belongs to the DP universality class.

Our purpose here is to apply the spreading dynamics to this map. First, we have to set the model in a synchronized state, i.e., the variables of both chains of CML's must take the same value. But despite that constraint there is a considerable freedom in doing that. Below we present results for two choices.

(i) Random synchronized state. In this case each pair of local variables takes a different random value, i.e., $u_1(x,0) = u_2(x,0) = r(x)$, where $0 \leqslant r(x) \leqslant 1$ and $r(x)$ varies from site to site.

(ii) Homogeneous synchronized state. In this case $r(x) = r$ and is constant for each x.

Let us note that when γ is large enough and model (1) reaches a synchronized state, this state is still chaotic. That is why the random synchronized states (i) are a much better approximation of such "natural" synchronized states. Later in this section we will see that the spreading dynamics confirms such an observation.

Having set the model in the synchronized state we initiate activity by assigning at a randomly chosen site x_0 a new random number either for $u_1(x_0)$ or for $u_2(x_0)$. Then we monitor the time evolution, measuring $w(t)$. We always used the system size $L = 2t_m + 1$ where t_m is the maximum simulation time. In this way the spreading is never affected by finite size effects. Moreover, the data were averaged over $10^3 - 10^4$ independent runs. Final results shown in Figs. 1–3 are obtained for $\gamma = \gamma_c = 0.2875$. Off criticality the data deviate from the power-law behavior in a typical way. Estimating the asymptotic slope of our data, we conclude that for the random synchronized state the exponents are in good agreement with very accurately known DP values: $\delta_{DP} = 0.1595$, $\eta_{DP} = 0.3137$, and $z = 1.2652$ [15]. However, in the case of homogeneous synchronized states, the exponents η and δ are clearly different and we estimate $\delta = 0.43(1)$ and $\eta = 0.05(1)$.

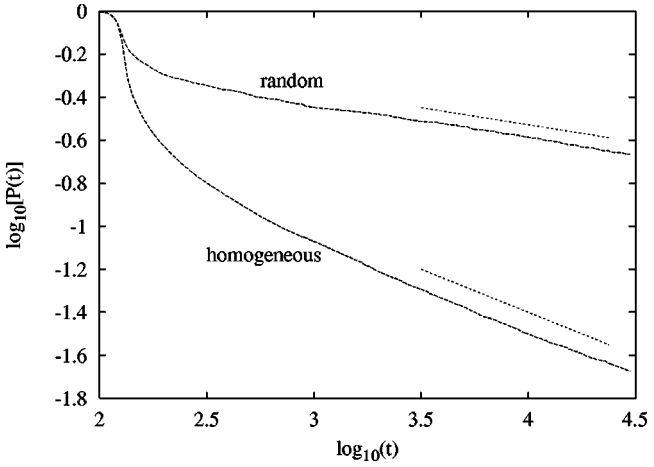

FIG. 1. The survival probability $P(t)$ for the Bernoulli map at $\gamma=\gamma_c=0.2875$ for random and homogeneous absorbing states as a function of time t. The slopes correspond to $\delta=0.1595$ (DP value) for the upper straight dotted line, and to $\delta=0.43$ for the lower one.

Let us note that a very similar situation occurs in certain models with infinitely many absorbing states, where these critical exponents are also found to depend on the choice of the absorbing state [13]. Although the spreading exponents are nonuniversal in this class of models, they obey the following relation:

$$\eta+\delta=\eta_{DP}+\delta_{DP}\,. \tag{4}$$

It turns out that the estimated exponents for homogeneous synchronized states also obey this relation within an estimated error. From Eq. (4) and the hyperscaling relation (3) it follows ($d=1$ in our case) that the exponent z must be constant and thus independent of the choice of the absorbing state. Indeed, in Fig. 3 one can see that for both the random and homogeneous absorbing states the asymptotic increase

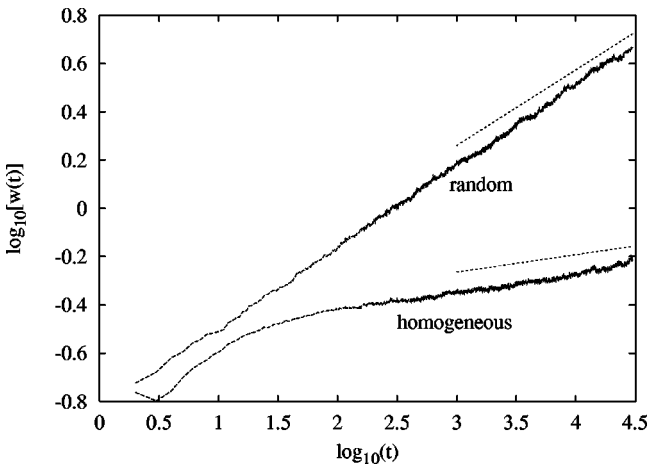

FIG. 2. The averaged difference $w(t)$ as a function of time t for the Bernoulli map at $\gamma=\gamma_c=0.2875$ and for random and homogeneous absorbing states. The upper straight dotted line has a slope that corresponds to the DP value $\eta=0.3134$, and for the lower straight line $\eta=0.05$.

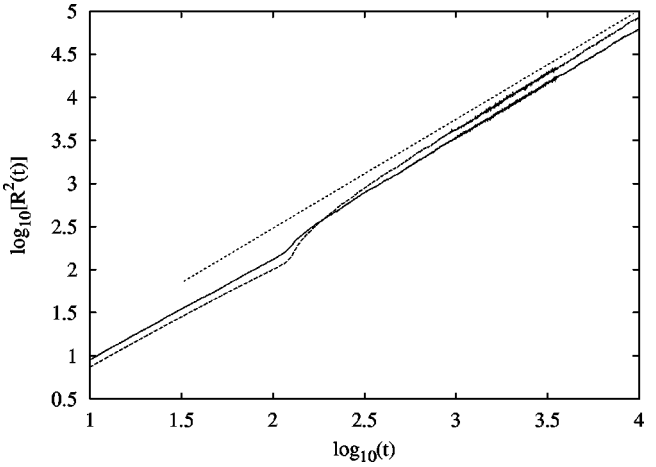

FIG. 3. The average square spread $R^2(t)$ as a function of time t for the Bernoulli map at $\gamma=\gamma_c=0.2875$ with random (solid line) and homogeneous (dashed line) absorbing states. The straight dotted line has a slope that corresponds to the DP value $z=1.2652$.

of $R^2(t)$ is described by the same exponent that most likely takes the DP value $z=1.2652$.

For models with infinitely many absorbing states it is also known that the spreading exponents for so-called natural absorbing states coincide with the DP exponents. Briefly, the natural absorbing states are the ones that are reached by the dynamics of a given model. Since the spreading exponents for random synchronized states coincide with DP exponents, one obtains that such states are very close to the natural synchronized states. On the other hand, as expected, the dynamics of homogeneous synchronized states (ii) is much different from the natural and random ones.

The main conclusion which follows from the above calculations is that synchronization should be considered as a transition in a model with multiple absorbing states rather than a single one. Except for non-DP values of η and δ it has essentially no other consequences in the one-dimensional

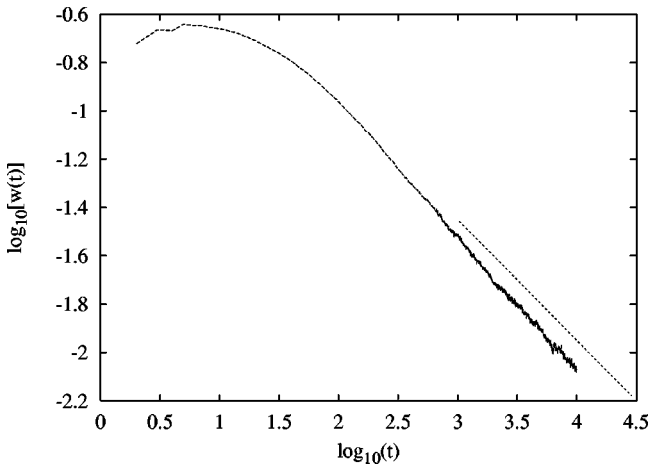

FIG. 4. The averaged difference $w(t)$ as a function of time t for the symmetric tent map at $\gamma=\gamma_c=0.176\ 14$ and for random absorbing states. The least-square fit to the last decade data gives $\eta=-0.53(5)$. The dotted straight line has a slope that corresponds to $\eta=-0.5$.

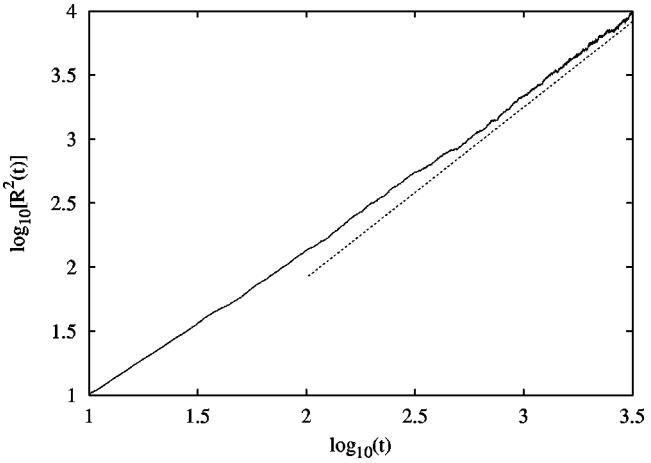

FIG. 5. The average square spread $R^2(t)$ as a function of time t for the symmetric tent map at $\gamma=\gamma_c=0.176\ 14$ and random absorbing states. The straight dotted line has a slope that corresponds to the KPZ value $z=1.3333$.

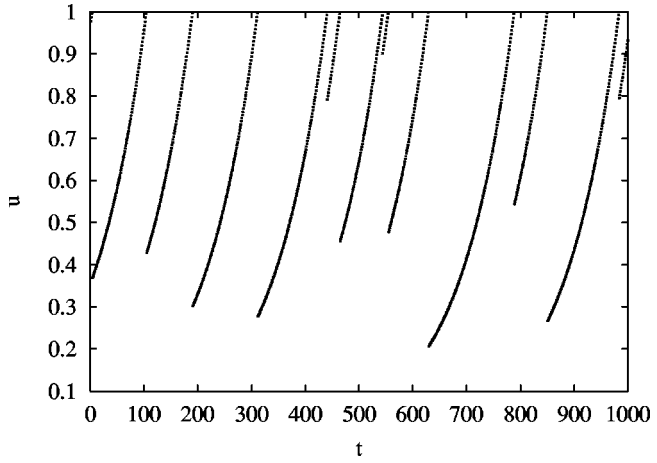

FIG. 7. The plot of successive iterations of the asymmetric tent map (5) for $a=1.01$. Most of the time is spent on the gradually increasing (laminar) part, occasionally interrupted by irregular jumps.

case. For example, all steady-state exponents keep the DP values. However, the situation might be different in higher-dimensional models with infinitely many absorbing states. In particular, there are some analytical and numerical indications that in such a case a non-DP criticality might appear [16].

B. Symmetric tent map

The second map examined by AP is the symmetric tent map defined as $f(u)=1-2|u-1/2|$ $(0\leqslant u\leqslant 1)$. In this case they found that the synchronization transition belongs to the BKPZ universality class and occurs at $\gamma=\gamma_c=0.176\ 14(1)$. A qualitative difference between the critical behavior in the case of Bernoulli and tent maps is attributed to the strong nonlinearity (i.e., discontinuity) of the first map.

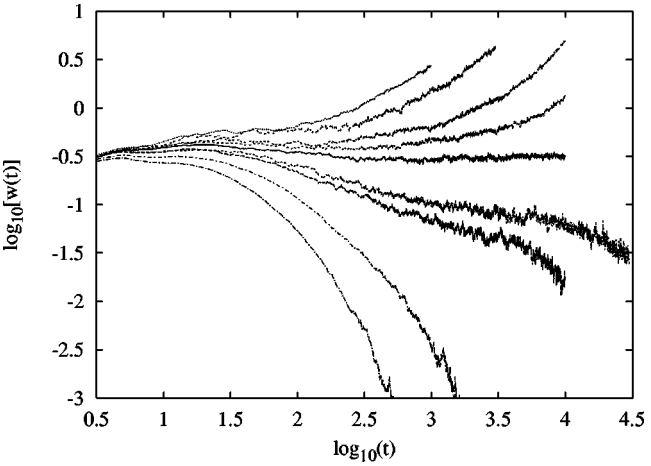

FIG. 6. The averaged difference $w(t)$ as a function of time t for the symmetric tent map with homogeneous absorbing states. Calculations were done for (from top) $\gamma=0.17$, 0.172, 0.174, 0.175, 0.176 14 (critical), 0.178, 0.18, 0.185, and 0.19. For $\gamma<0.176\ 14$ $w(t)$ asymptotically increases linearly in time while it decreases faster than a power law for $\gamma>0.176\ 14$.

Another interesting feature reported by AP is a different behavior of the transverse Lyapunov exponent $\lambda_\perp$. For the tent map $\lambda_\perp$ vanishes exactly at γ_c, while for the Bernoulli map it vanishes inside a chaotic phase. In this case the correct order parameter is the finite amplitude propagation velocity [9,17].

For the tent map we also performed the spreading dynamics calculations. For the random synchronized states our results for the time dependence of $w(t)$ are shown in Fig. 4. The asymptotic decay of $w(t)$ is described by the exponent $\eta=-0.53(5)$ (note the minus sign). As for the estimation of δ, our results strongly suggest that in this case $\delta=0$. Indeed, in the examined range of the threshold p we observed that all runs survived until the maximum measured time $t_m=10^4$. Most likely such a value of δ is related to the fact that in this

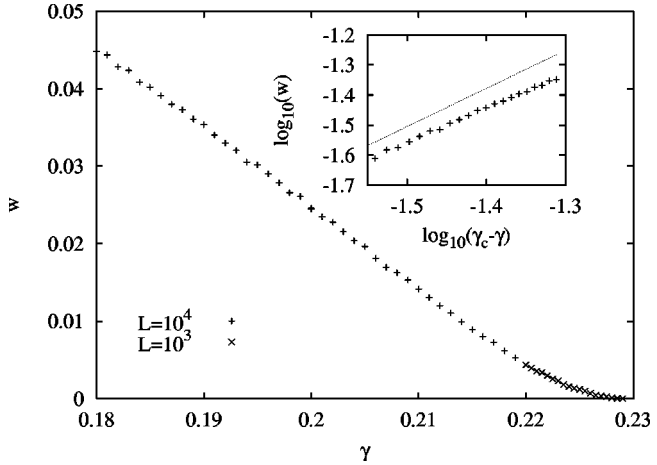

FIG. 8. The steady-state synchronization error w as a function of γ for the asymmetric tent map $(a=1.1)$. The measurement was made during $t=10^5$ steps after 5×10^4 steps of relaxation. In the range $(0.22\leqslant\gamma\leqslant\gamma_c=0.2288)$ w is well fitted by a power-law function $a(\gamma_c-\gamma)^\beta$, where $\beta=1.5$. In the logarithmic scale (inset) these data are better fitted with $\beta=1.3$ (dotted line) but a slight bending toward a greater value of β can also be seen.

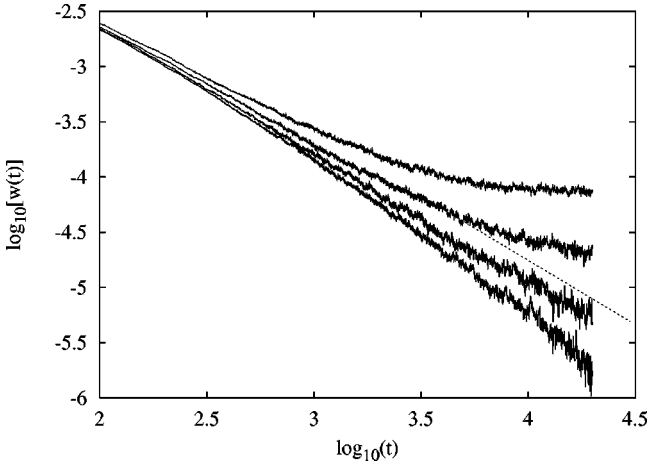

FIG. 9. The time dependence of w for the asymmetric tent map ($a=1.1$) and γ equal to (from top) 0.228, 0.2285, 0.2288 (critical), and 0.229. Calculations were done for $L=3\times10^5$. The dotted straight line has a slope corresponding to $\Theta=1.16$.

case also the Lyapunov exponent vanishes at the critical point. From the behavior of $R^2(t)$ (Fig. 5) we estimate $z=1.30(5)$, which is in good agreement with the expected KPZ value $z=\frac{4}{3}$ [8,18].

The hyperscaling relation provides a constraint on the exponents η, δ, Θ, and z. Since for the BKPZ universality class z is a simple number (4/3), it is tempting to assume that other exponents are also simple numbers. Thus we might speculate that in this model the exact value of η is -0.5. Then, from the hyperscaling relation (3) together with $\delta=0$ and $z=\frac{4}{3}$ we obtain $\Theta=\frac{7}{6}=1.166\ldots$. Such a value might be compared with numerical estimations of this exponent, which range from 1.1(1) [8,18] to 1.26(3) [10]. Let us also note that our estimation of the exponents η and δ is consistent with the estimation based on the numerical solution of a certain Langevin equation that belongs to the same universality class [19].

We also performed spreading dynamics simulations with homogeneous synchronized states. At criticality ($\gamma=0.176\ 14$) $w(t)$ seems to remain constant in time (Fig. 6), and that implies $\eta=0.0$. Moreover, we estimate in this case $\delta=0.0(1)$ and $z=0.85(10)$. Such values of spreading exponents do not satisfy the hyperscaling relation (3). The reason for such a disagreement is not clear to us. Let us note, however, that for hyperscaling to hold, a number of scaling assumptions must be satisfied [14]. One cannot exclude that homogeneous absorbing states are ''too unnatural'' for these assumptions to hold. Nevertheless, spreading dynamics in this case most likely correctly locates the critical point (Fig. 6). Further investigation of this problem is left for the future.

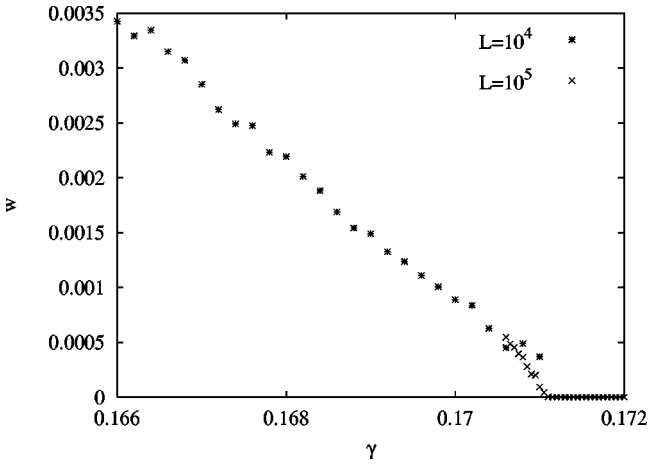

FIG. 10. The steady-state synchronization error w as a function of γ for the asymmetric tent map ($a=1.02$). The measurement was made during $t=10^5$ steps after 5×10^4 steps of relaxation.

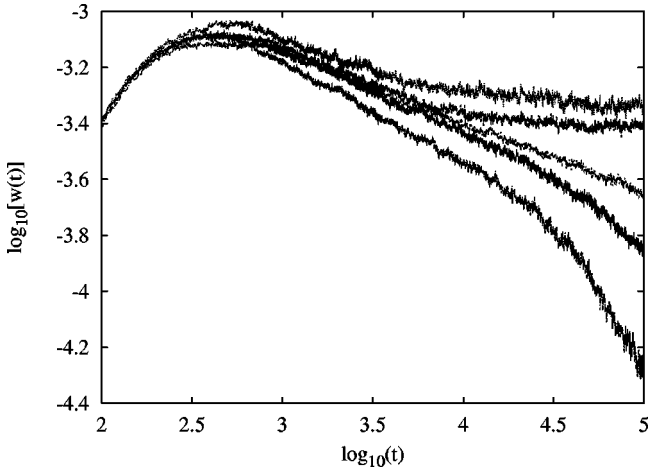

FIG. 11. The time dependence of w for the asymmetric tent map ($a=1.02$) and γ equal to (from top) 0.1707, 0.1709, 0.170 95, 0.1710, and 0.1712. Calculations were done for $L=5\times10^4$. We identify the central curve as critical.

C. Asymmetric tent map

In this subsection we examine the asymmetric tent map defined as

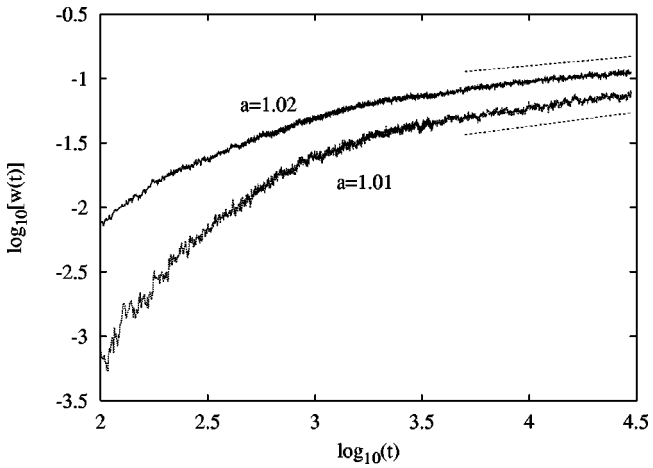

FIG. 12. The averaged difference $w(t)$ as a function of time t for the asymmetric tent map and for random absorbing states. Calculations were done for $a=1.02$ with $\gamma=\gamma_c=0.170\ 95$ and for $a=1.01$ with $\gamma=\gamma_c=0.136\ 95$. The dotted straight lines have a slope that corresponds to $\eta=0.15$ (upper) and $\eta=0.22$ (lower).

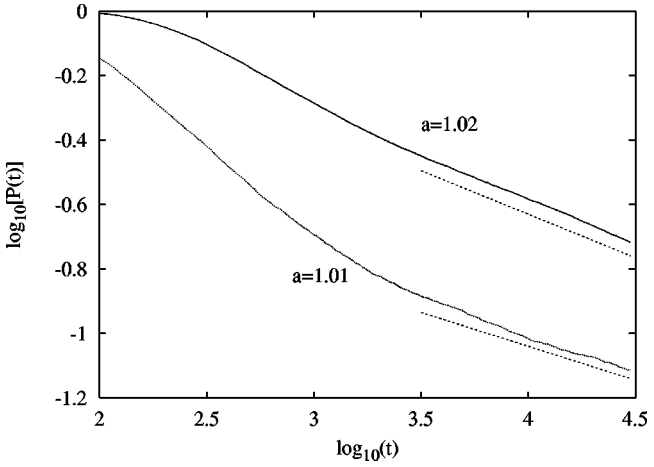

FIG. 13. The survival probability $P(t)$ for the asymmetric tent map with random absorbing states. Calculations were done for $a=1.02$ with $\gamma=\gamma_c=0.170\,95$ and for $a=1.01$ with $\gamma=\gamma_c=0.136\,95$. The dotted straight lines have a slope that corresponds to $\Theta=0.27$ (upper) and $\Theta=0.21$ (lower).

$$f(u)=\begin{cases} au & \text{for } 0\leqslant u<1/a, \\ a(1-u)/(a-1) & \text{for } 1/a\leqslant u\leqslant 1, \end{cases} \tag{5}$$

and $1<a\leqslant 2$. For $a=2$ this is the symmetric tent map. Let us notice that in the limit $a\to 1$, the slope of the second part of this map diverges. Moreover, the first part approaches the identity function. For a only slightly greater than 1 it leads to an interesting intermittencylike behavior that is shown in Fig. 7. A simple argument show that in the limit $a\to 1$ the average length of the laminar part τ diverges as $\tau\sim 1/(a-1)$. Indeed, approximately τ equals the number of iterations needed for the map to reach unity; namely, we have $u_0 a^{\tau}=1$, where u_0 is the initial value. Thus we obtain $\tau=-\ln(u_0)/\ln(a)\sim 1/(a-1)$. The appearance of a characteristic time τ that diverges for $a\to 1$, as we will see, causes

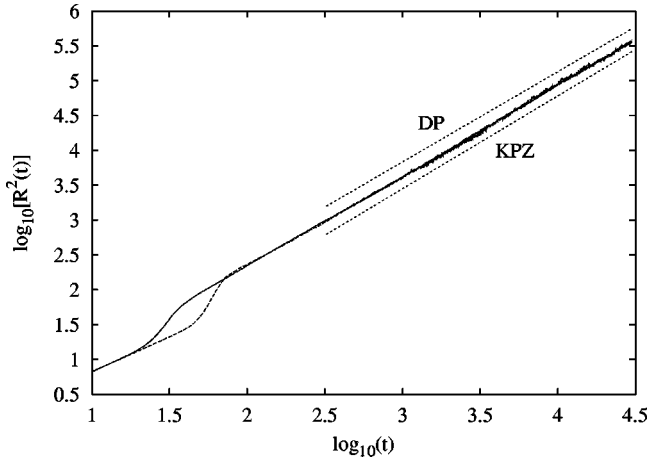

FIG. 14. The average square spread $R^2(t)$ as a function of time t for the asymmetric tent map and random absorbing states. Calculations were done for $a=1.02$, $\gamma=\gamma_c=0.170\,95$ (solid line) and $a=1.01$, $\gamma=\gamma_c=0.136\,95$ (dashed line). The straight dotted lines have slopes that correspond to the DP and KPZ values of z.

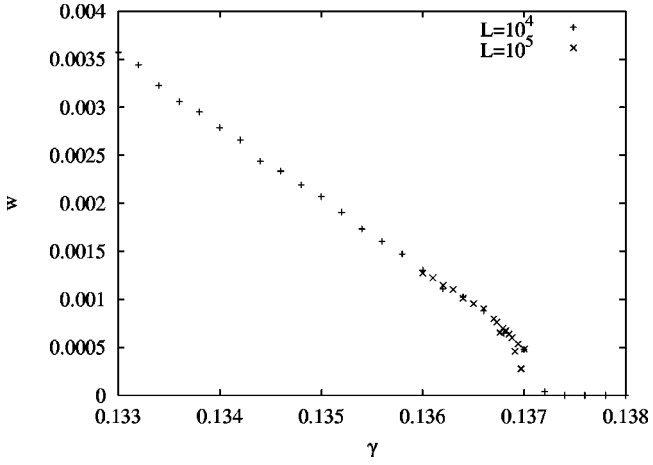

FIG. 15. The steady-state synchronization error w as a function of γ for the asymmetric tent map ($a=1.01$). The measurement was made during $t=10^5$ steps after 5×10^4 steps of relaxation.

some numerical difficulties already for a close to 1. Below we present the results of our calculations for $a=1.1$, 1.02, and 1.01.

1. a=1.1

When a is not too close to 1, model (1) remains in the BKPZ universality class. In particular, for $a=1.1$ the estimated exponents $\beta=1.4(2)$ (Fig. 8) and $\Theta=1.16(10)$ (Fig. 9) are in good agreement with other estimations for this universality class.

2. a=1.02

However, for a close to 1 the nature of the transition changes. From the measurements of w (Fig. 10) and its time dependence $w(t)$ (Fig. 11), we estimate that in this case $\gamma_c=0.170\,95$ and $\Theta=0.25(5)$. Using the spreading dynamics calculations for the random synchronized states at the critical point we estimate (Figs. 12–14) $\eta=0.15(3)$, $\delta=0.27(2)$,

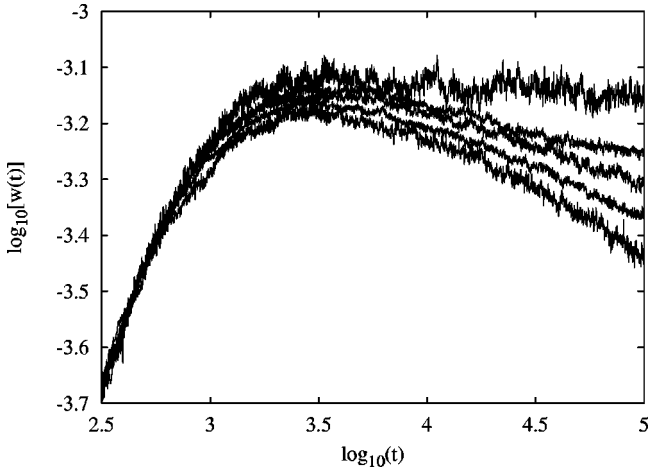

FIG. 16. The time dependence of $w(t)$ for the asymmetric tent map ($a=1.01$) and γ equal to (from top) 0.1368, 0.136 85, 0.1369, 0.136 95, and 0.137. Calculations were done for $L=5\times 10^4$.

TABLE I. Critical parameters for the symmetric and asymmetric tent maps. For $a=2$ the model belongs to the BKPZ universality class. The last column shows how much the critical exponents deviate from the hyperscaling relation (3).

a	γ_c	Θ	η	δ	β	z	$\eta+\delta$	$z/2-\Theta-\eta-\delta$
2								
(BKPZ)	0.176 14	1.26(3)	$-0.53(5)$	0.0(1)	1.50(5)	1.30(5)		0.07(0.11)
1.1	0.2288	1.16(10)			1.4(2)	1.30(5)		
1.02	0.170 95	0.25(5)	0.15(3)	0.27(2)		1.32(3)	0.42	0.01(0.11)
1.01	0.136 95	0.15(2)	0.22(2)	0.21(2)		1.25(5)	0.43	0.04(0.08)
DP		0.1595	0.3137	0.1595	0.2765	1.2652	0.4732	0

and $z=1.32(3)$. All of the exponents except z are far from the BKPZ values.

3. a=1.01

From the measurements of w (Fig. 15) and its time dependence $w(t)$ (Fig. 16), we estimate that in this case $\gamma_c=0.136\ 95$ and $\Theta=0.15(2)$. As for the $a=1.02$ results, our results for w close to the critical point are not sufficiently accurate to determine β. Using the spreading dynamics calculations for the random synchronized states at the critical point we estimate (Figs. 12–14) $\eta=0.22(2), \delta=0.21(2)$, and $z=1.25(5)$. Again, the exponents, except z, are far from the BKPZ values. However, Θ and z are consistent with the DP value. Moreover, the sum $\eta+\delta=0.43$ is also quite close to the DP value (0.4732). Thus, it is in our opinion likely that in this case the model belongs to the DP universality class but the random synchronized states are not natural synchronized states and that is why η and δ separately do not take their DP values. Let us note that for the Bernoulli map, examined in Sec. III A, the random synchronized states are probably a good approximation of the natural synchronized states, since the spreading exponents obtained coincide with the DP values. Most likely, for $a=1.01$ natural synchronized states include some sort of correlations that are clearly absent in our purely random construction of such states.

At first sight it seems that by taking a even closer to 1 we should retrieve DP exponents with a better accuracy. However, as can be seen in Fig. 12 or Fig. 13, for a getting closer and closer to 1, the critical scaling sets in only after a longer and longer time. Thus, examining, for example, $a=1.001$ seems to be beyond the reach of our present computational resources. In our opinion, the increasing time needed to reach the critical scaling might be related to the characteristic time scale τ that appears for a single map, as was already discussed at the beginning of this section.

Our numerical results are summarized in Table I.

IV. DISCUSSION

In this paper we used a spreading dynamics technique to examine the dynamical properties of CML models undergoing a synchronization transition. Our main results show that (i) the synchronized state is not unique and (ii) non-BKPZ critical behavior might appear for continuous maps. The latter result was already predicted by Baroni *et al.* [6]. One of the open questions that we leave for the future is why, for sufficiently asymmetric but continuous maps, the linear analysis, which leads to the relation with the BKPZ model, breaks down. Some aspects of this problem were already addressed in the literature as ''stable chaos'' [6,9]. For strongly asymmetric maps the (deterministic) noise is very large and this seems to be the only factor that might change the universality class. It is known that, depending on how the noise scales with the order parameter, Langevin-type models, which presumably describe our model at criticality and at a coarsed-grained level, might exhibit either DP or BKPZ critical behavior [20]. In particular, when the amplitude of noise scales linearly with the order parameter the model exhibits the BKPZ critical behavior but the DP one for square root scaling. Thus, the problem is to explain how a qualitatively different scaling of the noise in a Langevin-type model could emerge due to more quantitative changes (in asymmetry) in a coupled CML system. It is also tempting to expect that BKPZ and DP critical behaviors meet for a certain asymmetry value a_c $(1.1<a_c<1.01)$ at a different multicritical point. Our estimation of Θ for $a=1.02$ significantly deviates from both DP and BKPZ values, which might be an indication of such a critical point.

ACKNOWLEDGMENTS

This work was partially supported by the Swiss National Science Foundation and the Project No. OFES 00-0578 ''COSYC OF SENS.''

[1] H. Fujisaka and T. Yamada, Prog. Theor. Phys. **69**, 32 (1983); A. S. Pikovsky, Z. Phys. B: Condens. Matter **55**, 149 (1984); S. Boccaletti, J. Kurths, G. Osipov, D. I. Vallades, and C. S. Zhou, Phys. Rep. **366**, 1 (2002).

[2] R. Roy and K. S. Thornburg, Phys. Rev. Lett. **72**, 2009 (1994); H. G. Schuster *et al.*, Phys. Rev. A **33**, 3547 (1984); W. Wang *et al.*, Chaos **10**, 248 (2000).

[3] J. F. Heagy, T. L. Carroll, and L. M. Pecora, Phys. Rev. E **52**, R1253 (1996); A. Amengual *et al.*, Phys. Rev. Lett. **78**, 4379 (1997); S. Boccaletti *et al.*, *ibid.* **83**, 536 (1999).

[4] P. Grassberger, Phys. Rev. E **59**, R2520 (1999).

[5] *Theory and Applications of Coupled Map Lattices*, edited by

K. Kaneko (John Wiley & Sons, Chichester, U.K., 1993).
[6] L. Baroni, R. Livi, and A. Torcini, Phys. Rev. E **63**, 036226 (2001).
[7] A. S. Pikovsky and J. Kurths, Phys. Rev. E **49**, 898 (1994).
[8] Y. Tu, G. Grinstein, and M. A. Muñoz, Phys. Rev. Lett. **78**, 274 (1997).
[9] R. Kapral, R. Livi, G. L. Oppo, and A. Politi, Phys. Rev. E **49**, 2009 (1994); A. Politi, R. Livi, G. L. Oppo, and R. Kapral, Europhys. Lett. **22**, 571 (1993).
[10] V. Ahlers and A. S. Pikovsky, Phys. Rev. Lett. **88**, 254101 (2002).
[11] P. Grassberger, Z. Phys. B: Condens. Matter **47**, 365 (1982); H. K. Janssen, *ibid.* **42**, 151 (1981).
[12] P. Grassberger and A. de la Torre, Ann. Phys. (N.Y.) **122**, 373 (1979).
[13] J. F. F. Mendes, R. Dickman, M. Henkel, and M. C. Marques, J. Phys. A **27**, 3019 (1994).
[14] For a general introduction models with absorbing states, see, e.g., H. Hinrichsen, Adv. Phys. **49**, 815 (2000).
[15] I. Jensen, J. Phys. A **32**, 5233 (1999).
[16] F. van Wijland, Phys. Rev. Lett. **89**, 190602 (2002).
[17] F. Ginelli, R. Livi, and A. Politi, J. Phys. A **35**, 499 (2002). A. Torcini, P. Grassberger, and A. Politi, *ibid.* **28**, 4533 (1995).
[18] M. A. Muñoz and T. Hwa, Europhys. Lett. **41**, 147 (1998).
[19] W. Genovese and M. A. Muñoz, Phys. Rev. E **60**, 69 (1999).
[20] M. A. Muñoz, Phys. Rev. E **57**, 1377 (1998).